Glycoconjugate Journal (2023) 40:435–448
https://doi.org/10.1007/s10719-023-10121-y

RESEARCH

The generation of 5-*N*-glycolylneuraminic acid as a consequence of high levels of reactive oxygen species

Ruifeng Bai[1] · Jingyi Wang[1] · Inka Brockhausen[2] · Yin Gao[1]

Received: 13 December 2022 / Revised: 12 April 2023 / Accepted: 9 May 2023 / Published online: 2 June 2023

Abstract

The presence of *N*-glycolylneuraminic acid (Neu5Gc), a non-human sialic acid in cancer patients, is currently attributed to the consumption of red meat. Excess dietary red meat has been considered a risk factor causing chronic inflammation and for the development of cancers. However, it remains unknown whether Neu5Gc can be generated via a chemical reaction rather than via a metabolic pathway in the presence of high levels of reactive oxygen species (ROS) found in the inflammatory and tumor environments. In this study, the conversion of *N*-acetylneuraminic acid (Neu5Ac) to Neu5Gc has been assessed *in vitro* under conditions mimicking the hydroxyl radical-rich humoral environment found in inflammatory and cancerous tissues. As a result, Neu5Gc has been detected via liquid chromatography-multiple reaction monitoring mass spectrometry. Furthermore, this conversion has also been found to take place in serum biomatrix containing ROS and in cancer cell cultures with induced ROS production.

Keywords Sialic acid · 5-*N*-acetylneuraminic acid · 5-*N*-glycolylneuraminic acid · Reactive oxygen species · Cancer cells

Abbreviations

CE	collision energy
CMAH	*N*-acetylneuraminic acid hydroxylase
DCFH-DA	2',7'-dichlorodihydrofluorescein diacetate
DP	declustering potential
LC-Q-TRAP MS; LC-MRM	liquid chromatography-multiple reaction monitoring-mass spectrometry
Neu5Gc	RE%, Relative Error
ROS	reactive oxygen species
SA	sialic acid

Introduction

Sialic acid (SA) is a common terminal epitope of the glycan component found in glycoconjugates, which covers the surfaces of all vertebrate cells [1]. One of the key abnormalities observed in cancer is the up-regulation of sialylation, which is manifested by an elevated density of SA in cancer tissues and in the serum of cancer patients [1–5]. During cancer progression, the serum SA concentrations increased by 157 and 176 % during stage I and during stages II & III of cancer growth, respectively [4]. The detected SA level range in serum of colorectal cancer patients was 2.25-6.55 mM [5].

Another SA derivative is 5-*N*-glycolylneuraminic acid (Neu5Gc), which is characterized by an additional oxygen atom at the *N*-acetyl group of *N*-acetylneuraminic acid (Neu5Ac) (Fig. 1). Neu5Gc is thought to be endogenously synthesized in mammals due to the presence of the cytidine monophosphate-N-acetylneuraminic acid hydroxylase (CMAH) gene, which is responsible for catalyzing the hydroxylation reaction from Neu5Ac to Neu5Gc. However, humans lack a functional CMAH gene and cannot endogenously produce Neu5Gc [2]. Despite this, Neu5Gc has been detected in cancer patients and identified as a risk factor for causing cancer [6]. Therefore, the question regarding the origin of Neu5Gc in humans is of utmost importance.

Ruifeng Bai and Jingyi Wang authors contributed equally.

✉ Yin Gao
yingao@jlu.edu.cn

[1] Key laboratory for Molecular Enzymology and Engineering of Ministry of Education, School of Life Sciences, Jilin University, Changchun 130012, China

[2] Department of Biomedical and Molecular Sciences, Queen's University, Kingston, Ontario, Canada

The uptake of Neu5Gc from dietary sources such as red meat and animal organs and its subsequent metabolic incorporation into human glycoconjugates is a mechanism that currently explains the presence of this non-human SA in human cells [2]. Therefore, a public concern has been raised regarding a correlation between red meat consumption and an increased risk of developing cancer [7–13]. However, there is no evidence that proves a correlation between lower Neu5Gc levels and less cancer risk for vegetarians. Although vegetarians who consume dairy products may have higher Neu5Gc levels, strict vegetarians who avoid all animal products, including dairy, generally have lower levels of Neu5Gc in their diets. It is possible that additional mechanisms could still lead to the appearance of Neu5Gc in inflamed and cancerous tissues.

The production of reactive oxygen species (ROS) is upregulated in inflammation and cancer, and ROS promote many physiological and pathological aspects of malignant transformation and tumorigenesis [14–16]. Hydrogen peroxide (H_2O_2) is the most common form of ROS, and has been shown to be elevated in inflammatory and cancer tissues [17–22]. H_2O_2 is expressed at a higher level in tumor cells in comparison to normal cells and cancer cell lines [20, 21, 23]. Elevation of H_2O_2 concentrations (ie. 0.1 mM) can cause DNA damage, but cancer cells can sustain even higher H_2O_2 levels (eg. 10 mM) than healthy counterparts [24, 25] because tumor cells also synthesize antioxidant proteins, which balances the intracellular ROS levels and avoids oxidative stress-induced cell death, thus detoxifying the intracellular environment [26]. In inflammatory conditions, leukocytes release H_2O_2 when they are challenged with phorbol myristic acetate [18]. The upregulated H_2O_2 generation attracts more white blood cells recruited into the inflammatory site, as has been observed in a study on wounded zebrafish [17]. This scenario generates a gradient of H_2O_2 production that mediates rapid wound detection by immune cells. The local concentrations of H_2O_2 can be in the range of 0.5-50 µM, with the higher concentration observed closer to the wound.

Coincidentally, cancer patients were also found to exhibit elevated iron levels [27–32] that could contribute to the production of excess ROS. The total iron concentration is also related to the size and the stage of tumor, and iron concentrations that exceed 1.40 mg/ml (25 µM) are considered to be a risk factor for cancer.

In this paper, we propose a non-enzymatic reaction that converts Neu5Ac to Neu5Gc under conditions that parallel those found in inflammatory tissues and tumors, where elevated concentrations of H_2O_2 and iron(II) are present. The reaction conditions were designed to reflect the pH and reactant concentrations commonly found in both physiological and pathological conditions. We confirmed the production of Neu5Gc using ^{13}C-labelled Neu5Ac as a reactant. Furthermore, we were able to generate Neu5Gc in a human serum matrix through the addition of Neu5Ac, H_2O_2 and iron (II) under conditions similar to those in the buffer reactions. Finally, we analyzed the conversion of endogenous Neu5Ac to Neu5Gc in cultured lung cancer cells that were stimulated to generate ROS.

Materials and methods

Materials

Unless stated otherwise, the compounds, reagents and solvents employed herein were purchased from Sigma-Aldrich. The standard compounds: Neu5Ac and Neu5Gc were purchased from Tokyo Chemical Industry Co., Ltd. (TCI). *N*-acetyl-D-[2,3-$^{13}C_2$]neuraminic acid was purchased from Omicron Biochemical Inc. The internal standard (IS) D-glucuronic acid for mass spectrometry analysis was obtained from Solarbio, China. Iron(II) chloride (99.5% purity) was from Aladdin Industrial Corporation, China, ammonium acetate (analytical grade) from Sinopharm, China, acetonitrile (HPLC grade) from Fisher Chemical, USA and A549 lung cancer cells from ATCC. Milli-Q H_2O with a maximum resistivity of 18.2 Ω·cm at 25 °C, was prepared using a Milli-Q Water Purification System, Millipore, Bedford, MA, USA. The Anti-Neu5Gc Antibody Kit that contains purified anti-Neu5Gc antibody, chicken IgY isotype control and Neu5Gc assay blocking solution was purchased from BioLegend, USA. Goat anti-Chicken IgY (IgG)-FITC was from Absin, China. The fluorescent probe 2',7'-Dichlorofluorescein diacetate (DCF-DA) used for cellular ROS analysis was from Sigma-Aldrich.

Conversion of Neu5Ac to Neu5Gc in 50 mM ammonium acetate buffer pH 7.4

The concentrations of each reagent in different reaction mixtures are indicated in Table 2. Neu5Ac (1 mM) in 50 mM ammonium acetate pH 7.4 was used as a ***control solution*** to determine the concentration of Neu5Gc (an impurity) in the standard Neu5Ac. ***A blank solution*** contained 4 mM $FeCl_2$ and 4 mM H_2O_2 without Neu5Ac and was used to establish the background. Reaction mixtures were thoroughly mixed and incubated for 2 h at 37 °C, then quenched in ice-water bath followed by centrifugation at 16000×g for 3 min. The supernatant of each mixture was collected for analysis.

^{13}C-labelled Neu5Ac conversion in 50 mM ammonium acetate buffer pH 7.4

The reaction conditions are listed in Table 3. [2,3-$^{13}C_2$] Neu5Ac (1 mM) in 50 mM ammonium acetate pH 7.4 was

used as a ***control solution***. Reaction details are indicated in the section above.

Neu5Gc calibration curve

Standard Neu5Gc solutions were prepared as 1, 3, 10, 30, 100, 300, 500 ng/mL using the ***blank solution*** containing 100 ng/mL D-glucuronic acid as internal standard. Quality control (QC) Neu5Gc solutions with concentrations at 2.40, 24.0 and 400 ng/mL were also used as a further validation to evaluate the accuracy and precision of the calibration curve.

Sample preparation for MS analysis

Samples were diluted 10 times with H_2O containing internal standard D-glucuronic acid (100 ng/mL). All samples were extracted with a solid-phase extraction (SPE) column (Bond Elut PRS, Agilent, USA) before injecting into LC-Q-TRAP mass spectrometry. Prior to sample injection, the SPE columns were activated with 1 mL of methanol and equilibrated with 1 mL of H_2O. Samples were subsequently loaded onto the activated columns and the eluents were collected and placed into the auto-sampler.

Quantitative analysis of Neu5Gc

The ZORBAX Eclipse XDB-C18 column (4.6 × 100 mm, 5μm, Agilent, USA) was used as the separation column for reversed phase (RP) chromatography-multiple reaction monitoring-mass spectrometry (LC-MRM). The temperature of the auto-sampler was set to 25° C, and the sample injection volume was 20 μL. An aqueous solution containing 0.01 % ammonium acetate was employed as mobile phase A and acetonitrile was mobile phase B. The elution gradient settings were summarized in Supplementary Table S1. The post-column eluent was introduced directly into the electrospray ionization source of a Q-TRAP 5500 mass spectrometer equipped with an electrospray ionization source operated in the negative mode (SCIEX, Concord, Canada). The quantification of Neu5Gc generated in each buffer reaction was assessed via the multiple reaction monitoring (MRM) mode. The injection parameters were set as follows: source temperature = 550 °C, ion spray voltage = -4500 V, nebulizer gas (N_2) = 25 psi, heater gas (N_2) = 50 psi, and curtain gas = 25 psi. Data acquisition was controlled using Analyst 1.6.1 software. Linear least-squares regression of calibration curves with $1/x^2$ weighting was used to evaluate the linearity.

Quantitative analysis of Neu5Gc in buffer reactions

The concentration of Neu5Gc in each buffer reaction was determined via a methodologically confirmed LC-MRM quantitative method (the method validation is shown in Supplementary information). A standard calibration curve with 7 concentration points at 1, 3, 10, 30, 100, 300, 500 ng/mL was established. Weighted linear regression was applied with $1/x^2$ as a weighting factor. The linear correlation coefficient (r^2) of the regression equation exceeded 0.99 and the measured deviation (RE%) between the indicated concentration and calculated concentration at each point on the calibration curve as well as the QC samples ranged between +15% and -15% which are considered with acceptable accuracy. The exception was the lower limit of quantification (LLOQ) point (RE%) which ranged between +20% and -20% which are also acceptable. The calibration curve with acceptable accuracy can be used to calculate the amount of Neu5Gc generated in each reaction.

Conversion of Neu5Ac to Neu5Gc in serum biomatrix

The reactions with different concentrations of substrates prepared in human serum (Bio-Channel Biotechnology, Nanjing, China) are listed in Table 4. The reaction mixtures were mixed and incubated for 2 h at 37 °C, and then quenched in ice-water bath followed by ultrafiltration centrifugation at 1550×g for 10 min using a 100 kDa membrane (Microsep Advance Centrifugal Device, Pall Corporation, USA). The filtrate (50 μL) from each serum reaction was added to 150 μL solution of 0.25% ammonia in acetonitrile for further centrifugation at 16000×g for 3 min. The supernatants were collected for LC-MRM analysis.

Conversion of Neu5Ac to Neu5Gc in cell culture

A549 lung cancer cells were cultured in the F-12K medium with 10% fetal bovine serum (FBS) and 1% Penicillin/Streptomycin (P/S) at 37 °C in a 5% CO_2 atmosphere, and then seeded into a 24-well plate at a density of 1×10^6 cells per well. After 24 h of incubation, the culture medium was removed and the cells were washed twice with PBS. Growth medium was then added to cells without FBS and antibiotics, followed by methyl violet, H_2O_2 and $FeCl_2$. The generation of ROS was confirmed with DCFH-DA assay [50] after 2 h incubation as shown in Supplementary Fig. S4. Final concentrations of the substances applied to the cell culture to study the conversion of Neu5Ac to Neu5Gc were shown in Table S9. After a 24 h incubation, cell culture supernatants with secreted SA were collected (A). ***Sample A*** represented the cell culture medium collected after treatment, which contained secreted Neu5Ac and the newly generated Neu5Gc. Cells were further treated with 8 mU/ml neuraminidase (Sigma N7885) in serum free medium for 3 h, and the culture supernatants with enzyme-released SA were collected (B). ***Sample B*** contained the Neu5Ac and Neu5Gc removed by neuraminidase from cell surface glycoconjugates. Cells were then incubated on ice with lysis buffer, and finally the

cell lysis solution was collected (C). ***Sample C*** contained free Neu5Ac and Neu5Gc inside of cells. ***Solutions A***, ***B*** and ***C*** were centrifuged at 16000×g for 5 min. The supernatant (50 µL) from each solution was added to 150 µL solution of 0.25% ammonia in acetonitrile followed by a further centrifugation at 16000×g for 3 min. The supernatants were collected for LC-MS analysis.

Fluorescence analysis of ROS and immunofluorescence of Neu5Gc

A549 lung cancer cells (from ATCC) were cultured in the DMEM medium with 10% fetal bovine serum (FBS) and 1% Penicillin/Streptomycin (P/S) at 37 °C in a 5% CO_2 atmosphere, and then seeded into 12-well plates. After 24 h of incubation, the culture medium was removed and the cells were washed three times with PBS. Growth medium without FBS and antibiotics was added to cells, followed by treatments with methyl violet, H_2O_2 and $FeCl_2$ for 2 h at the final concentrations listed in Table S9. After incubation, cells were washed with PBS twice and then incubated with 10 µM DCFH-DA for 30 min. The fluorescence of ROS was analyzed with flow cytometry using excitation and emission wavelengths of 488 and 525nm, respectively. Fluorescence images of fixed cells were captured under an IX73 OLYMPUS microscope.

Cells were seeded into 12-well plates with a cell slider in each well and grown for 24 h. The cells were then treated according to the conditions in Table S9 for 2 h, with the addition of methyl violet, H_2O_2 and $FeCl_2$. After treatment, the cells were fixed with 4% paraformaldehyde for 10 min at room temperature (RT) and subsequently washed with PBST (PBS contains 1% tween 20). Each well was then sealed with Neu5Gc assay blocking solution at RT for 1 h, followed by overnight incubation with purified anti-Neu5Gc (Chicken Polyclonal IgY) at 4 °C (BioLegend, Anti-Neu5Gc Antibody Kit). On the second day, cells were washed three times with PBS and incubated with goat anti-chicken IgY(IgG)-FITC for 1 h at 37 °C. After three additional washes with PBS, the nuclei were stained with DAPI at room temperature for 1 min. Free DAPI was removed by washing with PBS. The immunofluorescence images of fixed cells were then captured under a LSM710 ZEISS microscope.

MS analysis of Neu5Gc from serum biomatrix and cell culture

The Hydrophilic Agilent Infinity Lab Poroshell 120 HILIC-Z column (2.1 × 100mm, 2.7 µm, P, Agilent, USA) with a pre-column was used to separate sialic acid from a biological matrix for hydrophilic interaction chromatography (HILIC)-LC-MRM. 10 mM ammonium acetate aqueous solution was used as mobile phase A and 10 mM ammonium acetate-10% water-90% acetonitrile was used as mobile phase B. The gradient elution settings are summarized in Supplementary Table S2. The sample injection volume was 4 µL and all other LC parameters and MS parameters were the same as described above in the section of "Quantitative analysis of Neu5Gc in buffer reactions". The quantity of Neu5Gc generated in each reaction can be quantitatively compared based on the area of the analyte peak.

Results

Qualitative analysis of Neu5Gc generated *in vitro*

The collision energy (CE) and the declustering potential (DP) values for both the analytes (Neu5Ac and Neu5Gc) and the internal standard (IS) D-Glucuronic acid are provided in Table 1. Negative electrospray ionization mode was employed, and the three most abundant daughter ions produced by D-glucuronic acid (*m/z* 193.0) were observed at *m/z* 113.0, 85.0 and 72.9 (Fig. 1A). Similarly, the most abundant daughter ions produced by Neu5Ac (*m/z* 308.1) were observed at *m/z* 87.0, 98.1 and 170.1 (Fig. 1B), while the most abundant daughter ions produced by [2,3-$^{13}C_2$]Neu5Ac (*m/z* 310.1) were *m/z* 89.0, 99.1 and 172.1 (Fig. 1C). Overall,

Table 1 Mass spectrometry parameters employed in the compound-related MRM mode

Compound	Parent ion (*m/z*)	Daughter ion (*m/z*)	CE (eV)	DP (V)
Neu5Ac	308.1	87.0	-25	-25
Neu5Gc	324.1	116.1	-21	-36
Neu5Gc	324.1	186.1*	-24	-36
[2,3-$^{13}C_2$]Neu5Ac	310.1	89.0	-36	-40
[2,3-$^{13}C_2$]Neu5Gc**	326.1	89.0	-36	-40
[2,3-$^{13}C_2$]Neu5Gc**	326.1	188.1***	-21	-40
D-Glucuronic acid	193.0	113.0	-18	-42

* The monitoring daughter ion of Neu5Gc

** The parent ion and daughter ion were predicted by non-isotopic labeled Neu5Gc

*** The monitoring daughter ion of [2,3-$^{13}C_2$]Neu5Gc

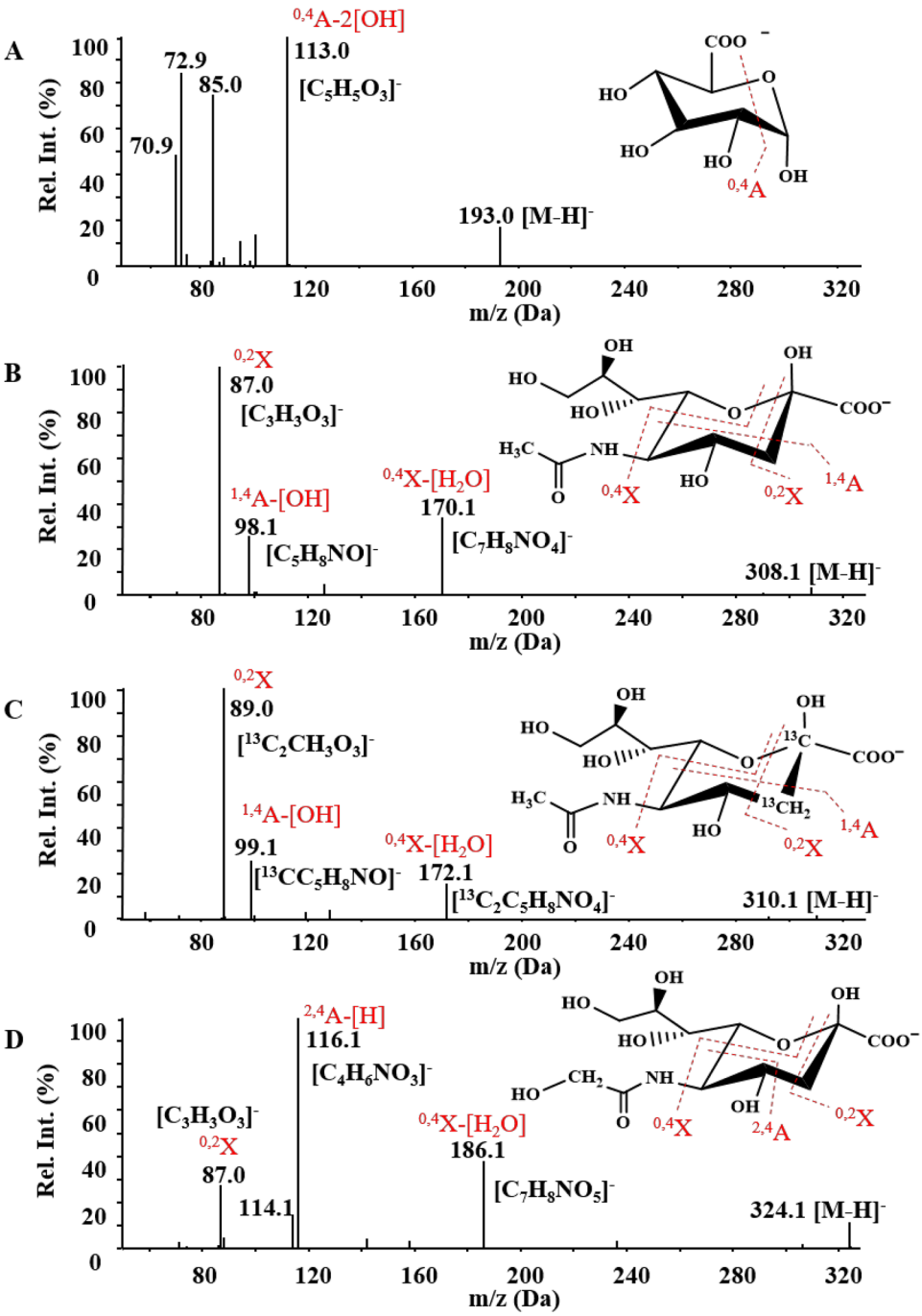

Fig. 1 The main daughter ions determined by MS-MS. **A** D-Glucuronic acid, **B** Neu5Ac, **C** [2,3-$^{13}C_2$] Neu5Ac and **D** Neu5Gc detected by electrospray ionization mass spectrometry in MS^2 mode with parent ions appearing at *m/z* 193.0, 308.1, 310.1 and 324.1, respectively

Fig. 1 shows the ion fragmentation pattern, which is consistent with previous literature [51]. The nomenclature of Domon and Costello was used to annotate the fragment ions [51]. In the case of Neu5Gc (*m/z* 324.1), the parent ions produced three daughter ions with the highest abundance appearing at *m/z* 116.1, 87.0, 186.1 (Fig. 1D). For quantification of Neu5Gc, the characteristic transition from *m/z* 324.1 to 116.1 and the fragment observed at *m/z* 186.1were employed as the daughter ions, and their abundance was monitored and quantified (Table 1). When acquiring MRM, the transition 323.9 ->115.9 was also acquired. The chromatographic peak representing Neu5Gc can only be accurately detected when both the transition 323.9 -> 115.9 and 324.1 -> 87.0 peaks appear simultaneously.

The ***buffer reactions 1-4*** and the ***control*** (Table 2) were injected into the LC-Q-TRAP MS. The *m/z* ratios of singly charged parent ions $[M-H]^-$ observed from standard solutions were very similar to the theoretical *m/z* values for Neu5Gc and the IS, respectively, as shown in Table 1. In the MRM mode, the various observed daughter ions that

Table 2 Concentrations of reactants in ammonium acetate buffer (pH 7.4) and analysis of the reaction product Neu5Gc. Reaction mixtures containing different concentration of Neu5Ac, $FeCl_2$ and H_2O_2 as indicated for 2 h at 37 °C. Reaction product analysis shows the mean concentration and yield of Neu5Gc ($n = 2$)

Buffer reactions	Reaction mixture (0.5 mL)			Reaction product analysis		
	Neu5Ac (mM)	$FeCl_2$ (mM)	H_2O_2 (mM)	Neu5Gc (μM)	Final Neu5Gc* (μM)	Yield (%)
Blank	-	4.000	4.000	0	-	-
Control	1.000	-	-	0.023	-	-
1	1.000	4.000	4.000	0.272	0.249	0.025
2	1.000	1.000	1.000	0.222	0.199	0.020
3	1.000	0.050	0.050	0.135	0.112	0.011
4	1.000	0.025	0.025	0.122	0.099	0.010

*Concentrations obtained by subtracting the endogenous (impurity) Neu5Gc from that of purchased Neu5Ac (Control)

arose from the Neu5Gc and the IS parent ions were consistent with those described in previous reports [33, 34]. The deviations between the retention times of chromatographic peaks corresponding to the analytes from the ***control*** and ***buffer reactions 1-4*** and to the Neu5Gc standard were within 1% (Relative Error, RE%). The MS spectra of the reaction samples demonstrated that ***buffer reactions 1-4*** generated a compound with very similar parent ions and fragment ions compared to those of the Neu5Gc standard. In addition, the *m/z* ion abundance ratios of the fragment ions relative to the molecular ion were within 20% of the ion ratios obtained for the Neu5Gc standards. Taken together, these results suggested that the reaction of Neu5Ac with H_2O_2 and iron (II) generated a product, which was confirmed to be Neu5Gc. The calibration curve and regression equation are shown in Supplementary Fig. S2, and the correlation coefficient r^2 was found to be 99.69%.

The Neu5Gc concentrations in the ***buffer reactions 1-4*** and the Neu5Ac to Neu5Gc conversion rates (Table 2) ranged between 0.01% and 0.025%. Figure 2 shows Neu5Gc intensity of the ***control*** and ***buffer reactions 1-4***, indicating that Neu5Ac has been converted to Neu5Gc in the presence of H_2O_2 and iron (II). The percentage yield was positively correlated with the concentrations of H_2O_2 and iron (II). The results indicated that the fold increase in H_2O_2/$FeCl_2$ concentration did not correspond to the same fold increase in Neu5Gc yield, suggesting the presence of other reactions. It should be noted that previous studies have described Neu5Ac as a hydrogen peroxide scavenger, as it can be oxidized in the presence of H_2O_2 [52, 53]. Thus, the increase in H_2O_2/$FeCl_2$ did not result in a proportional increase of Neu5Gc, possibly due to a higher proportion of decarboxylation reaction caused by the increased H_2O_2. The quantitative LC-Q-TRAP MS analysis used in this

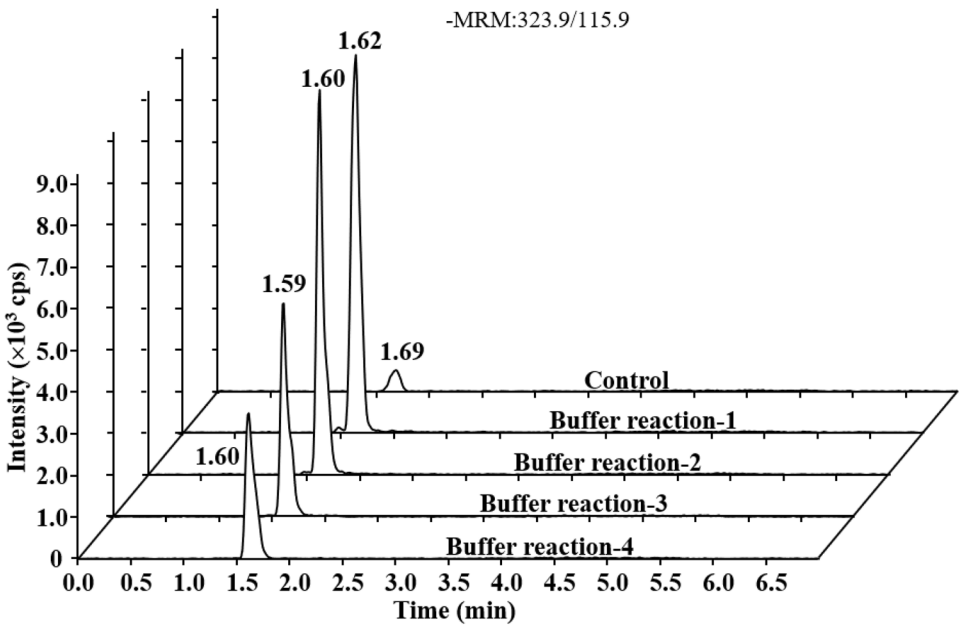

Fig. 2 The LC-MRM chromatograph of Neu5Gc in the control and buffer reaction-1 to 4. Reaction mixtures contained different concentrations of Neu5Ac, $FeCl_2$ and H_2O_2 as shown in Table 2. Buffer reaction-1: Neu5Ac (1.0 mM), $FeCl_2$ (4.0 mM), H_2O_2 (4 mM); Buffer reaction-2: Neu5Ac (1.0 mM), $FeCl_2$ (1.0 mM), H_2O_2 (1.0 mM).; Buffer reaction-3: Neu5Ac (1.0 mM), $FeCl_2$ (0.05 mM), H_2O_2 (0.05 mM); Buffer reaction-4: Neu5Ac (1.0 mM), $FeCl_2$ (0.025 mM), H_2O_2 (0.025 mM).The peak area of Neu5Gc increased with the increase in the concentration of reactants $FeCl_2$ and H_2O_2

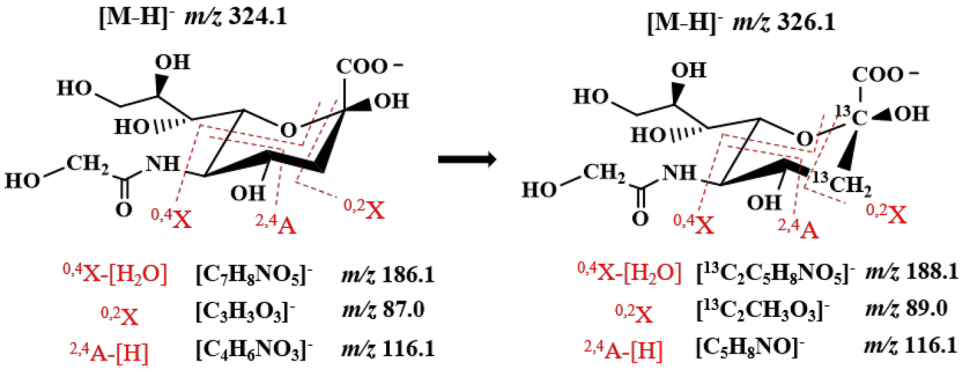

Fig. 3 The predicted daughter ion of [2,3-$^{13}C_2$]Neu5Gc according to the fragmentation pattern of Neu5Gc. The theoretical parent ion is *m/z* 326.1 and the predicted daughter ions are *m/z* 116.1, *m/z* 188.1 and *m/z* 89.0

study to determine the concentration of Neu5Gc has been validated using standard methodology (Supplementary information).

Proof of Neu5Ac to Neu5Gc conversion in buffer with ^{13}C-labelled Neu5Ac as a reactant

The characteristic conversion pattern from Neu5Ac to Neu5Gc was expected to be produced using ^{13}C-labelled 2,3-$^{13}C_2$]Neu5Ac. As seen in Fig. 3, fragment ion generated from *m/z* 326.1, could be *m/z* 89.0, 116.1 and 188.1. The product of [2,3-$^{13}C_2$]Neu5Gc was determined by extracting ion pair *m/z* 326.1/89.0 in MRM mode (Table 3). To analyze [2,3-$^{13}C_2$]Neu5Gc using MRM, we monitored the daughter ions m/z 188.1, 116.1, and 89.1, which were produced by the mother ion m/z 326.1 simultaneously. The chromatographic peak can only be identified as [2,3-$^{13}C_2$]Neu5Gc when all three peaks appear simultaneously, ensuring the accuracy of the detection.The original chromatogram is presented in Supplementary Fig. S3 (buffer reaction 5). Figure 4 shows [2,3-$^{13}C_2$]Neu5Gc intensity of the ***control*** and ***buffer reactions 5-7***, indicating that [2,3-$^{13}C_2$]Neu5Ac has been converted to [2,3-$^{13}C_2$]Neu5Gc in the presence of H_2O_2 and iron (II). Additionally, the intensity of [2,3-$^{13}C_2$]Neu5Gc ion was correlated with the concentrations of H_2O_2 and iron (II).

Comparisons of Neu5Gc generated in serum biomatrix reactions

Endogenous Neu5Gc was not detected in the serum background as shown by in Table 4 and Fig. 5. In the presence of H_2O_2 and iron(II) a significant amount of Neu5Gc was generated and the amount of Neu5Gc produced was correlated with the concentration of H_2O_2 and iron(II). These results suggested that Neu5Ac could react with hydroxyl radical to form Neu5Gc in human biofluids.

Analysis of Neu5Gc production in cell culture reactions

Lung cancer cells A549 grown in complete growth medium could endogenously produce Neu5Ac as well as Neu5Gc, although the supplement fetal bovine serum (FBS) contains a small amount of Neu5Gc, which was considered as a background during the analysis. Thus, no Neu5Ac was added as reactant in the cell culture reactions and all newly generated Neu5Gc was derived from Neu5Ac present in cell cultures. Cell culture conditions are listed in Table S9, and the ROS level in each cell culture condition was determined using the redox-sensitive fluorescent probe 2',7'-dichlorodihydrofluorescein diacetate (DCFH-DA) (Fig. S4). In the sample of

Table 3 Concentrations of reactants in ammonium acetate buffer pH 7.4. Reaction mixtures containing different concentration of [2,3-$^{13}C_2$] Neu5Ac, $FeCl_2$ and H_2O_2 as indicated for 2 h at 37 °C. Reaction product analysis shows the mean peak area of [2,3-$^{13}C_2$] Neu5Gc ($n = 2$)

Buffer Reactions	Reaction mixture (0.5 mL)			Reaction product analysis	
	[2,3-$^{13}C_2$] Neu5Ac (mM)	$FeCl_2$ (mM)	H_2O_2 (mM)	[2,3-$^{13}C_2$]Neu5Gc Peak Area (Counts)	[2,3-$^{13}C_2$]Neu5Gc Final Peak Area* (Counts)
Blank	-	4.000	4.000	0	-
Control	1.000	-	-	58100	-
5	1.000	1.000	1.000	4070000	4011900
6	1.000	0.050	0.050	2550000	2491900
7	1.000	0.025	0.025	938000	879900

*Final Peak Area obtained by subtracting the endogenous (impurity) [2,3-$^{13}C_2$]Neu5Gc from that of purchased [2,3-$^{13}C_2$]Neu5Ac (Control).

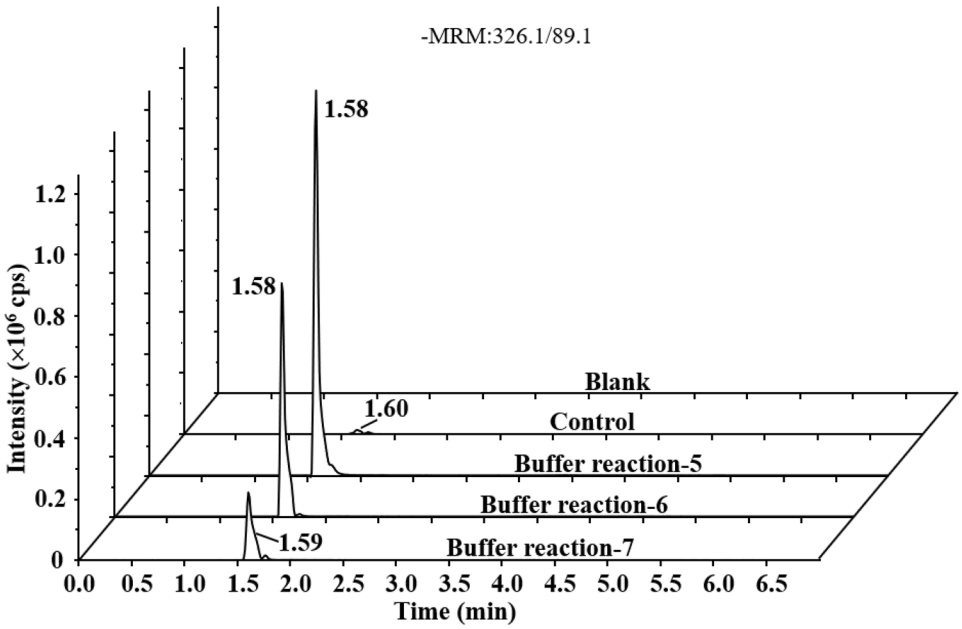

Fig. 4 The LC-MRM chromatograph of [2,3-$^{13}C_2$]Neu5Gc in the control and buffer reaction 5-7. Reaction mixtures contained different concentrations of [2,3-$^{13}C_2$]Neu5Ac, $FeCl_2$ and H_2O_2 as shown in Table 3. Buffer reaction-5: [2,3-$^{13}C_2$]Neu5Ac (1.0 mM), $FeCl_2$ (1.0 mM), H_2O_2 (1.0 mM); Buffer reaction-6: [2,3-$^{13}C_2$]Neu5Ac (1.0 mM), $FeCl_2$ (0.05 mM), H_2O_2 (0.05 mM).; Buffer reaction-7: [2,3-$^{13}C_2$]Neu5Ac (1.0 mM), $FeCl_2$ (0.025 mM), H_2O_2 (0.025 mM). The peak area of Neu5Gc increased with the increase in the concentration of reactants $FeCl_2$ and H_2O_2

cell culture-background (Table S9), the peak area ratio of Neu5Gc to Neu5Ac in solutions A, B and C together showed a total of 2.83%. In ***cell culture reactions 1 to 7***, the ratio of Neu5Gc to Neu5Ac (Table S9) was higher than the ratio in the ***cell culture-background***, suggesting that Neu5Gc was generated in cell cultures containing ROS-inducing agents and the amount of Neu5Gc production was correlated to the ROS level.

According to the cell culture preparations in Table S9, the ROS level in each condition was also determined with DCFH-DA assays. As seen in Fig. 6 there was increased fluorescence intensity in the presence of methyl violet, iron(II), and H_2O_2 in the ***cell culture reactions 1 to 11*** in comparison to the ***control***. The immunofluorescence assays carried out with anti-Neu5Gc antibody were used to assess the production of Neu5Gc in each cell culture condition (Table S9). The results indicated that increased Neu5Gc production was correlated with the concentration of ROS-inducing agents, methyl violet, H_2O_2 and iron(II) (Fig. 7) and associated with the ROS levels in cell cultures. These results further proved Neu5Gc can be converted from Neu5Ac, and the reaction was related to the ROS level.

Discussion

Neu5Gc has been associated with inflammation and cancers in condition of increased oxidative stress [35–39]. The underlying mechanisms of the expression of non-human Neu5Gc have been related to the consumption of Neu5Gc rich dietary sources. Previous studies have proposed multiple theories to explain the connection between red meat

Table 4 Concentrations of reactants in serum biomatrix and chromatographic peak area analysis of Neu5Gc in serum reactions. Reaction mixtures contain 60% serum and incubated with Neu5Ac, $FeCl_2$ and H_2O_2 as indicated for 2 h at 37 °C. Reaction product analysis shows the mean peak area of Neu5Gc and mean peak ratio of Neu5Gc vs. Neu5Ac ($n = 2$)

Serum reactions (0.5 mL)	Reaction mixture (0.5 mL)			Reaction product analysis		
	Neu5Ac (mM)	$FeCl_2$ (mM)	H_2O_2 (mM)	Neu5Gc Peak Area (Counts)	Neu5Gc Final Peak Area (Counts)*	Peak area ratio (‰) of Neu5Gc/Neu5Ac**
Background	-	-	-	0	-	-
Control	1.000	-	-	4060	-	-
Reaction-1	1.000	4.000	4.000	32200	28140	0.0247
Reaction-2	1.000	1.000	1.000	12200	8140	0.0071
Reaction-3	1.000	0.025	0.050	4170	110	0.0001

*Final Peak Area obtained by subtracting that of endogenous Neu5Gc from that of purchased Neu5Ac (Serum-control)

** The average peak area of exogenous Neu5Ac of Serum-control was 1.14×10^9 counts ($n = 4$)

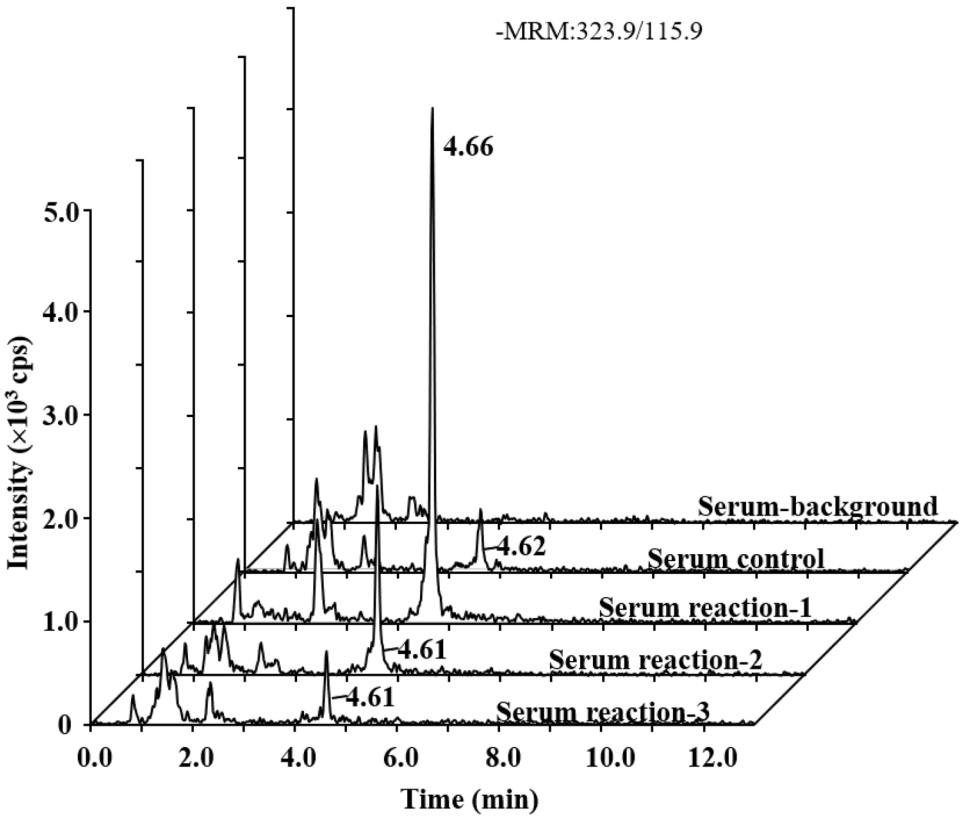

Fig. 5 The LC-MRM chromatograph of Neu5Gc in serum control and reaction-1 to 3 collected by Hilic-LC-MRM. Reaction mixtures contained 60% human serum and were incubated with different concentrations of Neu5Ac, $FeCl_2$ and H_2O_2 as indicated in Table 4. Serum reaction-1: Neu5Ac (1.0 mM), $FeCl_2$ (4.0 mM), H_2O_2 (4.0 mM); Serum reaction-2: Neu5Ac (1.0 mM), $FeCl_2$ (1.0 mM), H_2O_2 (1.0 mM).; Serum reaction-3: Neu5Ac (1.0 mM), $FeCl_2$ (0.025 mM), H_2O_2 (0.05 mM). The peak area of Neu5Gc increased with the increase in the concentration of reactants $FeCl_2$ and H_2O_2

consumption, inflammation and the risk of cancer. Firstly, extracellular free Neu5Gc and Neu5Gc-bearing glycoconjugates can be taken up by cultured cells via pinocytosis and enter lysosomes, where the Neu5Gc substituents of glycoproteins can be released via sialidase-mediated hydrolysis. The free Neu5Gc transported into the cytosol and subsequently

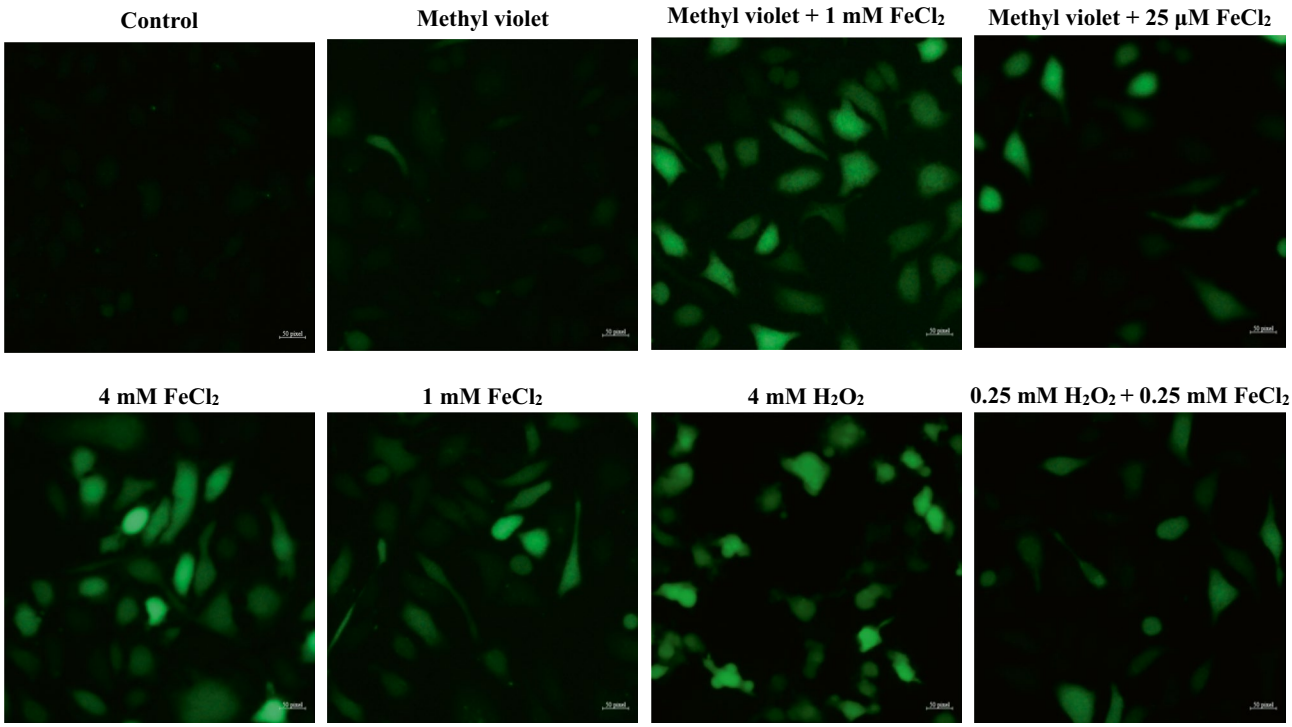

Fig. 6 Fluorescence of ROS at different reactant concentrations using DCFH-DA. Methyl violet, $FeCl_2$ and H_2O_2 were used to stimulate A549 cells to produce ROS. Cells were then incubated with DCFH-DA, and the intracellular ROS were determined via fluorescence microscope ($n = 3$). Scale bars, 50 pixel

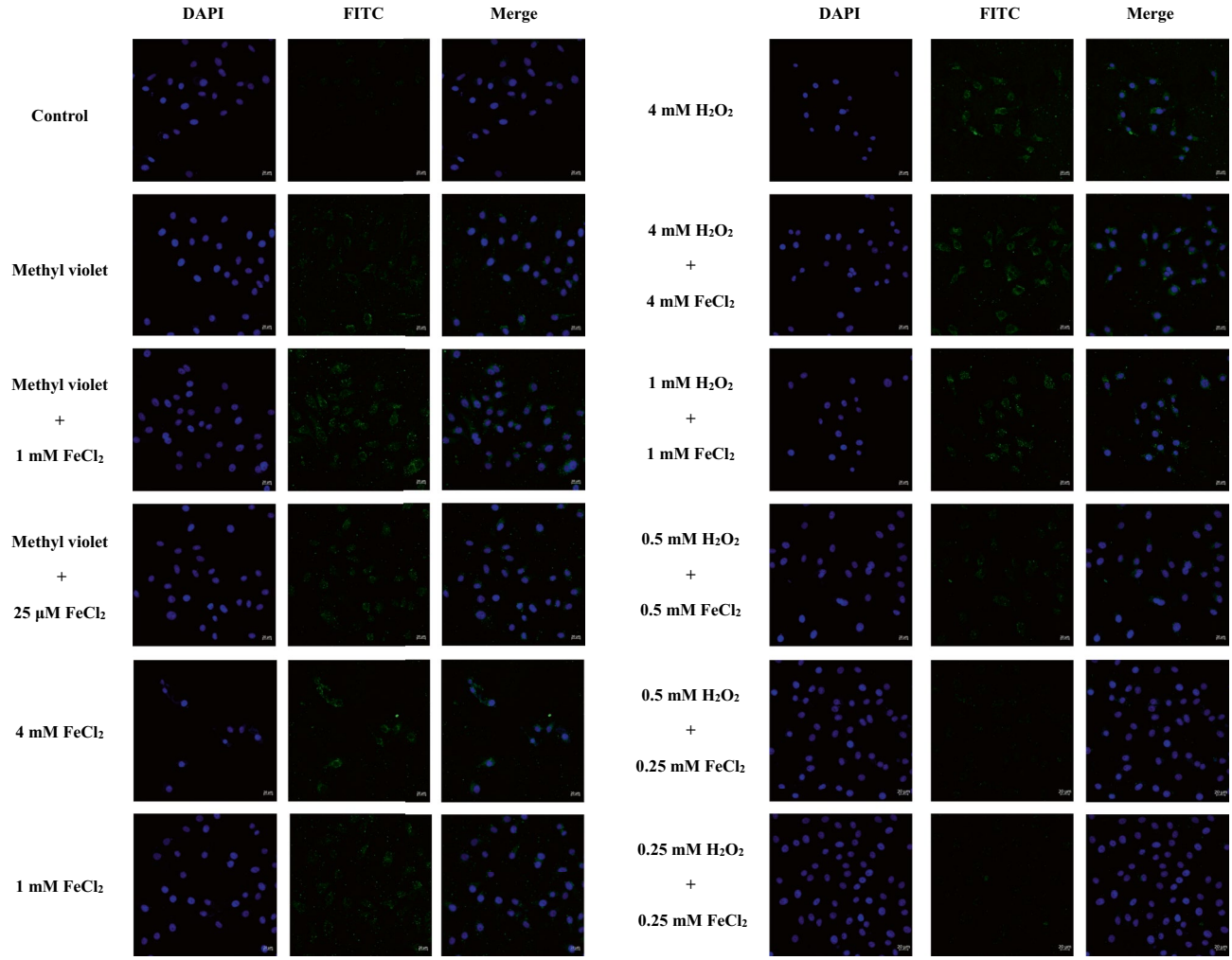

Fig. 7 Immunofluorescence of Neu5Gc at different reactant concentrations using anti-Neu5Gc antibody. DAPI (blue) and FITC (green) staining image of cells under different conditions. Neu5Gc level was determined by immunofluorescence method ($n = 3$). Scale bars were 20 μm

into the nucleus becomes activated to yield CMP-Neu5Gc, which is then used as a donor substrate in glycosylation reactions [11]. Secondly, CMAH-deficient mice that lack Neu5Gc have shown that the expression of Neu5Gc in tissues and various organs is related to meat consumption [40]. Thirdly, CMAH-deficient mice that were immunized against Neu5Gc showed a much higher incidence of hepatocellular carcinomas, along with evidence of Neu5Gc accumulation [7, 36]. Fourthly, studies in humans have further confirmed the link between dietary intake of Neu5Gc and the levels of serum anti-Neu5Gc IgG [54].

The other possibility is that Neu5Gc is generated by hydroxylation of the acetyl moiety of Neu5Ac under oxidative stress conditions, which is supported by our current LC-MRM data. Analyzing monosaccharide SA (Neu5Ac and Neu5Gc) is challenging due to low-molecular weight and negative effect of multiple hydroxyl groups in obtaining sufficient chromatographic retention, efficient separation and acceptable peak shape. In this study, a successful and validated LC-MRM method was established for Neu5Gc quantitative analysis (as shown in the Supplementary information) prior to the analysis of the *in vitro* conversion of Neu5Ac to Neu5Gc in buffer reactions (Fig. 2). Additionally, isotope-labelled Neu5Ac was applied in the buffer reaction to provide further evidence that Neu5Gc can be converted from Neu5Ac in the presence of oxidative factors (Fig. 4).

The percentage of Neu5Gc among all forms of SA in nature is typically less than 0.01%, but it has been found to increase in cancers [41]. Our results indicated that the percentage conversion from Neu5Ac to Neu5Gc in the buffer reactions containing ROS ranged between 0.01% and 0.025% (Table 2), which is consistent with previous quantitative studies of Neu5Gc levels in human cancer tissues (0.02-0.5%) and in an avian lymphoma cell line (0.03-0.11%) [42].

In buffer reactions, H_2O_2 can accept an electron from iron(II) via the Fenton reaction to produce a hydroxyl radical

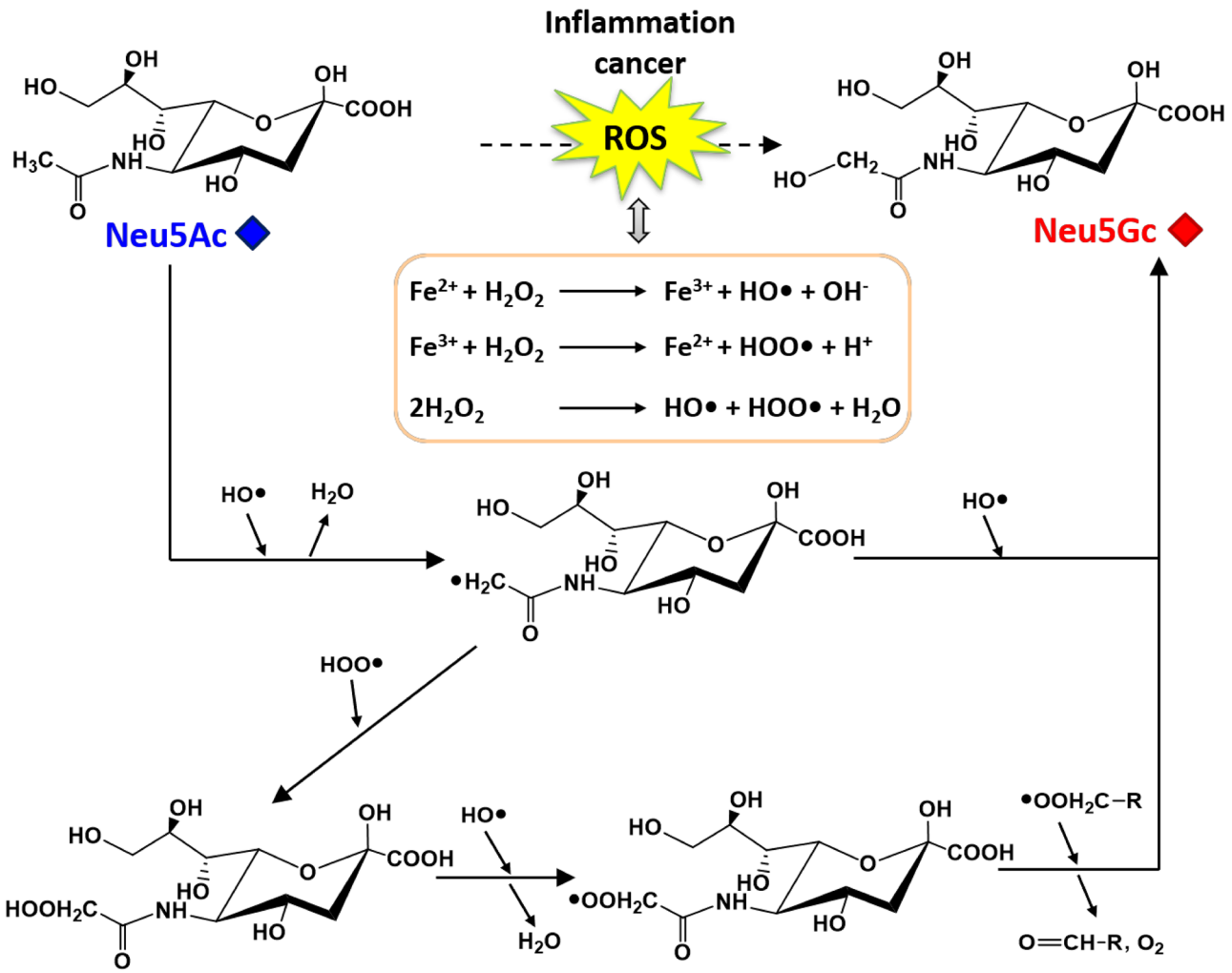

Fig. 8 Proposed conversion mechanism from Neu5Ac to Neu5Gc in the presence of ROS (HO• and HOO•). The CH_3 group in Neu5Ac can be oxidized to $\bullet CH_2$ in the presence of HO•, and $\bullet CH_2$ can further react with HO• to form the CH_2OH group in Neu5Gc. $\bullet CH_2$ also can form CH_2OOH with HOO•, and CH_2OOH can be further oxidized into $CH_2OO\bullet$ with HO•. With the presence of another $CH_2OO\bullet$, CH_2OH can be formed

(HO•) and a hydroxide ion. In this process, iron(III) can be reduced back to iron(II) with another molecule of H_2O_2, along with the production of a hydroperoxyl radical (HOO•) and a proton. Therefore, the net effect of the Fenton reaction is the deprotonation of H_2O_2 to generate two different ROS molecules (HO• and HOO•) along with a water molecule as a byproduct [26]. The CH_3 group in Neu5Ac can be oxidized to become $\bullet CH_2$ and further react with HO• / HOO• to form Neu5Gc. The proposed reaction mechanism of the conversion from Neu5Ac to Neu5Gc by HO• / HOO• is shown in Fig. 8. In pathological conditions, tumor cells can tolerate a high concentration of ROS via various mechanisms to detoxify the intracellular environment [26]. Thus, cancer cells maintain their oncogenic phenotype by carefully regulating the balance between intracellular ROS and antioxidant levels. The conversion of Neu5Ac to Neu5Gc may be another natural mechanism by which cancer cells consume ROS. However, in reaction 2, we observed a significant reduction in the production of Neu5Gc compared to the reduction of Neu5Ac, indicating the presence of other reactions. Increasing the amount of H_2O_2/$FeCl_2$ did not result in an equivalent increase in Neu5Gc, which may be attributed to a larger proportion of decarboxylation reaction resulting from the increased H_2O_2 [52, 53].

Human CMP-SA synthase is responsible for the synthesis of CMP-SA from SA and CTP, and the enzyme is equally active with Neu5Ac and Neu5Gc [43]. While less explored compared to acceptor substrate specificities, it is clear that human ST3GalI and ST6Gal can use unnatural CMP-SA with a modified N-acyl moiety [44]. Moreover, human ST6Gal can employ CMP-9-fluoresceinyl-NeuAc as donor substrate, exhibiting low K_m and high V_{max} relative

Table 5 Concentrations of reactants in A 549 lung cancer cell culture for fluorescence analysis of ROS and immunofluorescence assay of Neu5Gc. Cells were incubated with the reactants, methyl violet, $FeCl_2$ and H_2O_2 as indicated for 2 h at 37 °C (*n=3*)

Cell culture reactions	$FeCl_2$ (mM)	Methyl violet(mM)	Cell culture reactions	$FeCl_2$ (mM)	H_2O_2 (mM)
Control	-	-	6	-	4.000
1	-	3.000	7	4.000	4.000
2	1.000	3.000	8	1.000	1.000
3	0.025	3.000	9	0.500	0.500
4	4.000	-	10	0.250	0.500
5	1.000	-	11	0.250	0.250

to the natural CMP-Neu5Ac [45]. This could explain the elevated presence of Neu5Gc-containing antigens in cancers, such as sialyl-T(Neu5Gc), sialyl-Tn(Neu5Gc) [46, 47], sialyl-*N*-acetyllactosaminyl (Neu5Gc) chain and ganglioside GM3(Neu5Gc) (NeuGcα2,3Galβ1,4G1cβ1,1′Ceramide) [48]. Additionally, mammalian sialyltransferases purified from porcine, rat, and bovine tissues exhibit less donor specificity, allowing the utilization of CMP-Neu5Gc and CMP-Neu5Ac without preference [49].

To further support our hypothesis that hydroxylation of Neu5Ac could occur in biomatrix, the reactions were also performed in the human serum with the addition of H_2O_2 and iron(II). Results indicated that the generation of Neu5Gc from Neu5Ac occurred and correlated with the concentration of H_2O_2 and iron(II) (Tables 4 , 5 and Fig. 5).

A549 cells cultured with ROS inducing agent, including methyl violate [50], H_2O_2 and iron(II), were used to further confirm that the conversion of endogenous Neu5Ac to Neu5Gc can occur in cell culture [11]. As shown in Table S9, The results of ***cell culture reactions 1-7*** indicated that the generation of Neu5Gc from endogenous Neu5Ac correlated the concentration of ROS-inducing agents. This suggested that not only free Neu5Ac but also Neu5Ac in a glycosidic linkage can be converted to Neu5Gc due to elevated ROS levels.

Immunofluorescence assays were used to confirm the results obtained with LC-MRM analysis. As shown in Fig. 7, the fluorescence intensity increased with increasing concentrations of ROS-inducing agents. Therefore, Neu5Gc production is correlated with the ROS level in the cell cultures, indicating that Neu5Ac can be converted to Neu5Gc due to ROS elevation *in vivo*. These observations provide a new perspective for studying the mechanisms of Neu5Gc expression in various diseases. We also suggest a new mechanism for cancer cells to link high levels of ROS and hydroxylation, which could occur on Neu5Ac but potentially on other biological molecules as well.

Conclusions

The previous research has been shown that the expression of Neu5Gc in human cancer tissue and in blood plasma glycoproteins was related to red meat consumption. Our study proposes an additional possible mechanism that could lead to an increase in Neu5Gc expression in tumors and inflammatory tissue. The results of our study are based on quantitative LC-MRM analysis, which has been validated with the use of standard methodology. The *in vitro* buffer reactions have been designed to mimic physiological conditions, and the serum and cell culture experiments further support our findings. These *in vitro* data suggest that the conversion of Neu5Ac to Neu5Gc induced by ROS could also occur *in vivo*.

In the future, it would be important to test different iron-containing molecules, such as hemoglobin, myoglobin, and heme compounds, for their ability to convert Neu5Ac to Neu5Gc in the presence of ROS. Additionally, it will be crucial to investigate the possible conversion of CMP-Neu5Ac to CMP-Neu5Gc and hydroxylation of other carbohydrate molecules.

Supplementary Information The online version contains supplementary material available at https://doi.org/10.1007/s10719-023-10121-y.

Acknowledgements The authors thank Dr. Ying Xu and Dr. Xingze Qu (The Third Hospital, Jilin University) for the discussion of Fenton reaction. The authors thank Prof. Bo Wang (Department of Chemistry, Jilin University) for the discussion of the mechanism of hydroxylation reaction.

Author contributions Y.G. conceived and designed the experiments; R.B. and J.W. performed the experiments; Y.G., R.B. and J.W. analyzed the data; Y.G., R.B., J.W. and IB contributed to the preparation of the manuscript. All authors reviewed the manuscript.

Funding Y.G. thanks the Department of Science and Technology of Jilin Province, China [grant number 20200801066GH].

Declarations

Ethical Approval None.

Conflict of interest The authors declare that there is no conflict of interest regarding the publication of this article.

References

1. Pearce, O.M., Laubli, H.: Sialic acids in cancer biology and immunity. Glycobiology **26**, 111–128 (2016)
2. Varki, A.: Are humans prone to autoimmunity? Implications from evolutionary changes in hominin sialic acid biology. J. Autoimmun. **83**, 134–142 (2017)
3. Gruszewska, E., Cylwik, B., Panasiuk, A., Szmitkowski, M., Flisiak, R., Chrostek, L.: Total and free serum sialic acid concentration in liver diseases. Biomed. Res. Int. **2014**, 876096 (2014)

4. Paszkowska, A., Berbec, H., Semczuk, A., Cybulski, M.: Sialic acid concentration in serum and tissue of endometrial cancer patients. Eur. J. Obstet. Gynecol. Reprod. Biol. **76**, 211–215 (1998)
5. Feijoo, C., Paez, de la Cadena. M., Rodriguez-Berrocal, F.J., Martinez-Zorzano, V.S.: Sialic acid levels in serum and tissue from colorectal cancer patients. Cancer Lett. **112**, 155-160 (1997)
6. Varki, A.: N-glycolylneuraminic acid deficiency in humans. Biochimie **83**, 615–622 (2001)
7. Samraj, A.N., Pearce, O.M., Läubli, H., Crittenden, A.N., Bergfeld, A.K., Banda, K., Gregg, C.J., Bingman, A.E., Secrest, P., Diaz, S.L., Varki, N.M., Varki, A.: A red meat-derived glycan promotes inflammation and cancer progression. Proc. Natl. Acad. Sci. USA **112**, 542-547 (2015)
8. Deng, L.Q., Chen, X., Varki, A.: Exploration of Sialic Acid Diversity and Biology Using Sialoglycan Microarrays. Biopolymers **99**, 650–665 (2013)
9. Bergfeld, A.K., Pearce, O.M., Diaz, S.L., Lawrence, R., Vocadlo, D.J., Choudhury, B., Esko, J.D., Varki, A.: Metabolism of vertebrate amino sugars with N-glycolyl groups: incorporation of N-glycolylhexosamines into mammalian glycans by feeding N-glycolylgalactosamine. J. Biol. Chem. **287**, 28898–28916 (2012)
10. Bergfeld, A.K., Pearce, O.M., Diaz, S.L., Pham, T., Varki, A.: Metabolism of vertebrate amino sugars with N-glycolyl groups: elucidating the intracellular fate of the non-human sialic acid N-glycolylneuraminic acid. J. Biol. Chem. **287**, 28865–28881 (2012)
11. Bardor, M., Nguyen, D.H., Diaz, S., Varki, A.: Mechanism of uptake and incorporation of the non-human sialic acid N-glycolylneuraminic acid into human cells. J. Biol. Chem. **280**, 4228–4237 (2005)
12. Pan, A., Sun, Q., Bernstein, A.M., Schulze, M.B., Manson, J.E., Stampfer, M.J., Willett, W.C., Hu, F.B.: Red meat consumption and mortality: results from 2 prospective cohort studies. Arch. Intern. Med. **172**, 555–563 (2012)
13. Banda, K., Gregg, C.J., Chow, R., Varki, N.M., Varki, A.: Metabolism of vertebrate amino sugars with N-glycolyl groups: mechanisms underlying gastrointestinal incorporation of the non-human sialic acid xeno-autoantigen N-glycolylneuraminic acid. J. Biol. Chem. **287**, 28852–28864 (2012)
14. Liou, G.Y., Storz, P.: Reactive oxygen species in cancer. Free Radic Res **44**, 479–496 (2010)
15. Oktyabrsky, O.N., Smirnova, G.V.: Redox regulation of cellular functions. Biochemistry (Mosc) **72**, 132–145 (2007)
16. Nogueira, V., Hay, N.: Molecular pathways: reactive oxygen species homeostasis in cancer cells and implications for cancer therapy. Clin. Cancer Res. **19**, 4309–4314 (2013)
17. Niethammer, P., Grabher, C., Look, A.T., Mitchison, T.J.: A tissue-scale gradient of hydrogen peroxide mediates rapid wound detection in zebrafish. Nature **459**, 996–999 (2009)
18. Prowse, S.J., Michalski, W.P., Fahey, K.J.: Enhanced H2O2 release from immune chicken leucocytes following infection with Eimeria tenella. Immunol. Cell Biol. **70**(Pt 1), 41–48 (1992)
19. Driessens, N., Versteyhe, S., Ghaddhab, C., Burniat, A., De Deken, X., Van Sande, J., Dumont, J.E., Miot, F., Corvilain, B.: Hydrogen peroxide induces DNA single- and double-strand breaks in thyroid cells and is therefore a potential mutagen for this organ. Endocr. Relat. Cancer **16**, 845–856 (2009)
20. Szatrowski, T.P., Nathan, C.F.: Production of large amounts of hydrogen peroxide by human tumor cells. Cancer Res. **51**, 794–798 (1991)
21. Lim, S.D., Sun, C., Lambeth, J.D., Marshall, F., Amin, M., Chung, L., Petros, J.A., Arnold, R.S.: Increased Nox1 and hydrogen peroxide in prostate cancer. Prostate **62**, 200–207 (2005)
22. Song, Y., Driessens, N., Costa, M., De Deken, X., Detours, V., Corvilain, B., Maenhaut, C., Miot, F., Van Sande, J., Many, M.C., Dumont, J.E.: Roles of hydrogen peroxide in thyroid physiology and disease. J. Clin. Endocrinol. Metab. **92**, 3764–3773 (2007)
23. Lennicke, C., Rahn, J., Lichtenfels, R., Wessjohann, L.A., Seliger, B.: Hydrogen peroxide - production, fate and role in redox signaling of tumor cells. Cell Commun. Signal **13**, 39 (2015)
24. Lopez-Lazaro, M.: Dual role of hydrogen peroxide in cancer: possible relevance to cancer chemoprevention and therapy. Cancer Lett. **252**, 1–8 (2007)
25. O'Donnell-Tormey, J., DeBoer, C.J., Nathan, C.F.: Resistance of human tumor cells *in vitro* to oxidative cytolysis. J. Clin. Invest. **76**, 80–86 (1985)
26. Sullivan, L.B., Chandel, N.S.: Mitochondrial reactive oxygen species and cancer. Cancer Metab. **2**, 17 (2014)
27. Wen, C.P., Lee, J.H., Tai, Y.P., Wen, C., Wu, S.B., Tsai, M.K., Hsieh, D.P., Chiang, H.C., Hsiung, C.A., Hsu, C.Y., Wu, X.: High serum iron is associated with increased cancer risk. Cancer Res. **74**, 6589–6597 (2014)
28. Li, F., Kishida, T., Kobayashi, M.: Serum iron and ferritin levels in patients with colorectal cancer in relation to the size, site, and disease stage of cancer. J. Gastroenterol. **34**, 195–199 (1999)
29. Huang, X.: Iron overload and its association with cancer risk in humans: evidence for iron as a carcinogenic metal. Mutat. Res. **533**, 153–171 (2003)
30. Kucharzewski, M., Braziewicz, J., Majewska, U., Gozdz, S.: Selenium, copper, and zinc concentrations in intestinal cancer tissue and in colon and rectum polyps. Biol. Trace Elem. Res. **92**, 1–10 (2003)
31. Pardoe, H., Clark, P.R., St Pierre, T.G., Moroz, P., Jones, S.K.: A magnetic resonance imaging based method for measurement of tissue iron concentration in liver arterially embolized with ferrimagnetic particles designed for magnetic hyperthermia treatment of tumors. Magn. Reson. Imaging **21**, 483–488 (2003)
32. Hornik, P., Milde, D., Trenz, Z., Vysloužil, K., Stužka, V.: Colon tissue concentrations of copper, iron, selenium, and zinc in colorectal carcinoma patients. Chemical Papers **60**, 297–301 (2006)
33. Pearce, O.M., Varki, A.: Chemo-enzymatic synthesis of the carbohydrate antigen N-glycolylneuraminic aci:d from glucose. Carbohydr. Res. **345**, 1225–1229 (2010)
34. Wang, F., Xie, B., Wang, B., Troy, F.A. 2nd.: LC-MS/MS glycomic analyses of free and conjugated forms of the sialic acids, Neu5Ac, Neu5Gc and KDN in human throat cancers. Glycobiology **25**, 1362-1374 (2015)
35. Samraj, A.N., Laubli, H., Varki, N., Varki, A.: Involvement of a non-human sialic Acid in human cancer. Front. Oncol. **4**, 33 (2014)
36. Hernandez, A.M., Toledo, D., Martínez, D., Griñán, T., Brito, V., Macías, A., Alfonso, S., Rondón, T., Suárez, E., Vázquez, A.M., Pérez, R.: Characterization of the antibody response against NeuGcGM3 ganglioside elicited in non-small cell lung cancer patients immunized with an anti-idiotype antibody. J. Immunol. **181**, 6625–6634 (2008)
37. Taylor, R.E., Gregg, C.J., Padler-Karavani, V., Ghaderi, D., Yu, H., Huang, S., Sorensen, R.U., Chen, X., Inostroza, J., Nizet, V., Varki, A.: Novel mechanism for the generation of human xeno-autoantibodies against the nonhuman sialic acid N-glycolylneuraminic acid. J. Exp. Med. **207**, 1637–1646 (2010)
38. Shathili, A.M., Brown, H.M., Everest-Dass, A.V., Tan, T.C.Y., Parker, L.M., Thompson, J.G., Packer, N.H.: The effect of streptozotocin-induced hyperglycemia on N-and O-linked protein glycosylation in mouse ovary. Glycobiology **28**, 832–840 (2018)
39. Mwangi, D.W., Bansal, D.D.: Evidence of free radical participation in N-glycolylneuraminic acid generation in liver of chicken treated with gallotannic acid. Indian J. Biochem. Biophys. **41**, 20–28 (2004)
40. Hedlund, M., Tangvoranuntakul, P., Takematsu, H., Long, J.M., Housley, G.D., Kozutsumi, Y., Suzuki, A., Wynshaw-Boris, A., Ryan, A.F., Gallo, R.L., Varki, N., Varki, A.: N-glycolylneuraminic acid deficiency in mice: implications for human biology and evolution. Mol. Cell Biol. **27**, 4340–4346 (2007)

41. Hokke, C.H., Bergwerff, A.A., van Dedem, G.W., van Oostrum, J., Kamerling, J.P., Vliegenthart, J.F.: Sialylated carbohydrate chains of recombinant human glycoproteins expressed in Chinese hamster ovary cells contain traces of N-glycolylneuraminic acid. FEBS Lett. **275**, 9–14 (1990)
42. Kawai, T., Kato, A., Higashi, H., Kato, S., Naiki, M.: Quantitative determination of N-glycolylneuraminic acid expression in human cancerous tissues and avian lymphoma cell lines as a tumor-associated sialic acid by gas chromatography-mass spectrometry. Cancer Res. **51**, 1242–1246 (1991)
43. Mertsalov, I.B., Novikov, B.N., Scott, H., Dangott, L., Panin, V.M.: Characterization of Drosophila CMP-sialic acid synthetase activity reveals unusual enzymatic properties. Biochem. J. **473**, 1905–1916 (2016)
44. Noel, M., Noel, M., Gilormini, P.A., Cogez, V., Yamakawa, N., Vicogne, D., Lion, C., Biot, C., Guérardel, Y., Harduin-Lepers, A.: Probing the CMP-Sialic Acid Donor Specificity of Two Human beta-d-Galactoside Sialyltransferases (ST3Gal I and ST6Gal I) Selectively Acting on O- and N-Glycosylproteins. Chembiochem. **18**, 1251–1259 (2017)
45. Gross, H.J., Sticher, U., Brossmer, R.: A highly sensitive fluorometric assay for sialyltransferase activity using CMP-9-fluoresceinyl-NeuAc as donor. Anal Biochem **186**, 127–134 (1990)
46. Mortezai, N., Behnken, H.N., Kurze, A.K., Ludewig, P., Buck, F., Meyer, B., Wagener, C.: Tumor-associated Neu5Ac-Tn and Neu5Gc-Tn antigens bind to C-type lectin CLEC10A (CD301, MGL). Glycobiology **23**, 844–852 (2013)
47. Devine, P.L., Clark, B.A., Birrell, G.W., Layton, G.T., Ward, B.G., Alewood, P.F., McKenzie, I.F.: The breast tumor-associated epitope defined by monoclonal antibody 3E1.2 is an O-linked mucin carbohydrate containing N-glycolylneuraminic acid. Cancer Res. **51**, 5826-5836 (1991)
48. Padler-Karavani, V., Yu, H., Cao, H., Chokhawala, H., Karp, F., Varki, N., Chen, X., Varki, A.: Diversity in specificity, abundance, and composition of anti-Neu5Gc antibodies in normal humans: potential implications for disease. Glycobiology **18**, 818–830 (2008)
49. Higa, H.H., Paulson, J.C.: Sialylation of glycoprotein oligosaccharides with N-acetyl-, N-glycolyl-, and N-O-diacetylneuraminic acids. J. Biol. Chem. **260**, 8838–8849 (1985)
50. Jaroonwitchawan, T., Chaicharoenaudomrung, N., Namkaew. J., Noisa. P.: Curcumin attenuates paraquat-induced cell death in human neuroblastoma cells through modulating oxidative stress and autophagy. Neurosci. Lett. **636**, 40-47 (2017)
51. Seo, N., Ko, J., Lee, D., Jeong, H., Oh, M.J., Kim, U., Lee, D.H., Kim, J., Choi, Y.J., An, H.J.: In-depth characterization of non-human sialic acid (Neu5Gc) in human serum using label-free ZIC-HILIC/MRM-MS. Anal Bioanal Chem. **413**(20), 5227–5237 (2021)
52. Iijima, R., Takahashi, H., Namme, R., Ikegami, S., Yamazaki, M.: Novel biological function of sialic acid (N-acetylneuraminic acid) as a hydrogen peroxide scavenger. FEBS Lett. **561**(1–3), 163–6 (2004)
53. Neyra, C., Paladino, J., Le Borgne, M.: Oxidation of sialic acid using hydrogen peroxide as a new method to tune the reducing activity. Carbohydr Res. **11**(386), 92–8 (2014)
54. Bashir S, Fezeu LK, Leviatan Ben-Arye S, Yehuda S, Reuven EM, Szabo de Edelenyi F, Fellah-Hebia I, Le Tourneau T, Imbert-Marcille BM, Drouet EB, Touvier M, Roussel JC, Yu H, Chen X, Hercberg S, Cozzi E, Soulillou JP, Galan P, Padler-Karavani V. Association between Neu5Gc carbohydrate and serum antibodies against it provides the molecular link to cancer: French NutriNet-Santé study. BMC Med. **18**(1), 262 (2020)